Valeology: International Journal of Medical Anthropology and Bioethics
(ISSN 2995-4924) VOLUME 03 ISSUE 8, 2025

TOPICAL GOLD–CERIUM OXIDE NANOCOMPOSITE HYDROGEL PROMOTES REDOX HOMEOSTASIS AND WOUND REPAIR IN STREPTOZOTOCIN-INDUCED DIABETIC RATS: A CONTROLLED EXPERIMENTAL STUDY

Muna Khalifa Ali
Department of Physiology and Medical Physics, College of Medicine, Fallujah University, Iraq

Abstract:

Diabetic wounds are characterized by persistent oxidative stress, low-grade inflammation, and impaired matrix remodelling, which culminate in delayed closure and high rates of infection, amputation, and mortality. Redox-active nanomaterials such as cerium oxide and gold nanoparticles offer a rational strategy to intercept reactive oxygen species and rebalance pro- and anti-inflammatory signalling at the wound interface. This preclinical study evaluated a topically applied gold–cerium oxide ($Au–CeO_2$) nanocomposite hydrogel as an adjunctive therapy for cutaneous wound repair in streptozotocin-induced diabetic rats. After induction and stabilization of diabetes, standardized full-thickness dorsal excisional wounds were created and animals were randomized to receive either a nanoparticle-free hydrogel base or the $Au–CeO_2$ nanocomposite hydrogel once daily for up to 21 days. Macroscopic wound contraction and time to complete epithelialization were quantified from serial planimetric measurements. At predefined endpoints, wound tissue was harvested to assess oxidative stress (malondialdehyde, reduced glutathione, and antioxidant enzymes), inflammatory cytokines (TNF-α, IL-1β, IL-6), pro-healing mediators (VEGF, TGF-β1), and matrix remodelling markers (MMP-9, TIMP-1, hydroxyproline). Systemic oxidative stress indices, circulating cytokines, routine clinical chemistry, and haematological parameters were also measured, and a subset of rats underwent biomechanical testing of healed skin. Data were summarized as mean ± SD and compared between groups using Welch's unequal-variance independent-samples t-test. $Au–CeO_2$ hydrogel treatment significantly accelerated wound contraction at all time points and shortened epithelialization by nearly four days relative to the hydrogel base ($p < 0.001$). Treated wounds showed lower lipid peroxidation and pro-inflammatory cytokines, higher antioxidant capacity and pro-angiogenic growth factors, a more favourable MMP-9/TIMP-1 profile with

increased hydroxyproline, and superior mechanical strength of the repair tissue, without evidence of systemic toxicity. These findings support Au–CeO_2 nanocomposite hydrogel as a promising redox-modulating platform for enhancing diabetic wound healing. Further dose optimization, mechanistic exploration, and comparative studies against established advanced dressings are warranted in diabetic models.

Introduction

Introduction

Diabetic foot ulcers (DFUs) remain one of the most debilitating complications of diabetes, driven by persistent oxidative stress, low-grade inflammation, microbial colonization, and impaired angiogenesis, all of which converge to lock wounds in a non-resolving inflammatory phase and predispose to amputation and mortality (Wang et al., 2025). In this complex microenvironment, conventional dressings and systemic therapies often fail to adequately modulate redox homeostasis or provide sustained bioactive cues, prompting intensive interest in nanotechnology-enabled local drug delivery systems. Recent work has highlighted polymeric nanomedicines as versatile platforms capable of co-delivering antioxidants, growth factors, and antimicrobial agents in a controlled manner to diabetic wounds (Chen et al., 2025). Complementary reviews emphasize that advanced delivery systems—particularly nanoparticle-loaded hydrogels, nanofibers, and hybrid scaffolds—offer improved retention at the wound bed and better alignment with the dynamic requirements of DFU management (Yadav et al., 2025; Xiao et al., 2024).

Among inorganic nano-therapeutics, cerium oxide (CeO_2) nanoparticles occupy a unique position because of their switchable Ce^{3+}/Ce^{4+} redox couple, which confers potent, catalytic scavenging of superoxide and peroxides together with oxygen-modulating and anti-inflammatory effects. Recent reviews have consolidated preclinical evidence that CeO_2 nanoformulations can attenuate oxidative damage, normalize inflammatory signaling, and promote re-epithelialization and neovascularization in acute and chronic wounds, including diabetic models (Chen et al., 2024; Nosrati et al., 2023). Building on this concept, a ligand–metal charge-transfer–enhanced CeO_2 nanozyme was recently engineered to integrate potent reactive oxygen species (ROS) scavenging with antibacterial activity, achieving accelerated closure and improved granulation tissue in diabetic infected wounds (Wu et al., 2025).

Hydrogels are particularly attractive carriers for such redox-active nanomaterials because they can mimic the high-water content and viscoelasticity of native extracellular matrix while enabling sustained local release. For example, a double-network hydrogel reinforced with SS31-loaded mesoporous polydopamine nanoparticles combined photothermal antibiofilm activity with mitochondrial protection to restore full-thickness wound healing in diabetic rats (Deng et al., 2023). Similarly, a silk-based nanocomposite hydrogel that targets mitochondria has been shown to rebalance immune responses and redox status in diabetic wounds, underscoring the importance of concurrently addressing oxidative stress and inflammation (Chen et al., 2024).

Recent design trends also favor multifunctional hydrogels that couple robust mechanical support with intrinsic antibacterial and antioxidant functions. An “adobe-inspired” core–shell fiber hydrogel, for instance, achieved durable hemostasis, infection control, and sustained peptide release in diabetic wounds (Li et al., 2025). In parallel, a chitosan/hyaluronic acid hydrogel co-loaded with gold nanoparticles and fibroblast growth factor significantly enhanced re-epithelialization, collagen deposition, and neovascularization in diabetic rats, illustrating the regenerative potential of gold-based nanocomposites when integrated into a moist, bioactive matrix (Liu et al., 2024). Furthermore, ROS-scavenging lipid nanoparticle–mRNA formulations have demonstrated that precise modulation of the oxidative milieu can profoundly accelerate diabetic wound repair (Wang et al., 2024).

Collectively, these advances suggest that combining catalytically active CeO_2 nanozymes with pro-regenerative metallic nanoparticles in an injectable or topical hydrogel could provide an efficient strategy to restore redox balance, dampen inflammation, and support matrix remodeling in DFUs. However, there is still limited in vivo evidence on whether a topical gold–CeO_2 nanocomposite hydrogel can simultaneously correct local oxidative stress, normalize inflammatory and fibrotic mediators, and improve systemic redox indices in streptozotocin-induced diabetic models. The present study addresses this gap by systematically evaluating the impact of a topical Au–CeO_2 nanocomposite hydrogel on wound closure kinetics, tissue redox homeostasis, cytokine profiles, and biochemical parameters in diabetic rats.

The aim of the current research was to test the therapeutic value of topical use of a gold–cerium oxide nanocomposite hydrogel as a wound repair agent in streptozotocin-induced diabetic rats. Its main objective was whether the use of the nano-composite of Au nano-crystals and CeO_2 into a biocompatible hydrogel base improved the wound healing rate of the hydrogel base alone on the case of the standardized full-thickness excisional wounds. In this respect, the research evaluated the percentage wound area contraction with time and biomechanical strength of the repaired tissue as functional factors of better repair. The rationale was that, the Au–CeO_2 hydrogel would increase wound contraction interval, reduce wound complete re epithelialization duration, and generate healed skin with higher tensile strength compared to the wounds treated with control.

In addition to this central line of therapeutic inquiry, the paper was also aimed at mechanistic elucidation of any therapeutic benefit upon healing through questioning local states of redox and inflammatory-pro-healing signalling to the wound space. The study thus compared the oxidative stress and oxidant defense parameters in wound tissues by using indices of lipid peroxidation and the activity of major activity antioxidant enzymes, whereby it was hoped that treatment with the Au–CeO_2 hydrogel would be linked to reduced levels of oxidative injury, and increased endogenous antioxidant activity. Simultaneously, the concentrations of the selected pro-inflammatory cytokines and pro-healing mediators as well as the indicators of extracellular matrix deposition and remodelling were tested to identify whether the Au–CeO_2 formulation modified the local milieu to become more regenerative and less chronically inflamed.

Another objective of the research was to test the hypothesis as to whether there were quantifiable systemic effects of the local topical use of the Au–CeO_2 hydrogel on oxidative stress and inflammation in diabetic rats. Systemic biochemical indicators such as indicators of oxidative status, and circulating inflammatory cytokines were evaluated at intervals during the treatment process to this end. It was also hoped that any introduction of local redox modulation of the wound site would be manifested in a partial reduction in the systemic oxidative and inflammatory load in the diabetic host. Lastly, the efficacy of the Au–CeO_2 hydrogel topped on his back was local and systemic safety and tolerability in repeated administration when used topically as the objective of the study. The evaluation of clinical observations, alterations in body weight, routine haematological and biochemical parameters, and gross view on major organs was performed with anticipation of that no clinically related toxicity would be linked to the tested formulation. All these goals were established to pin these redox modulation and inflammatory regulation to structural and functional endpoints of wound repair thus offering a holistic evaluation of the Au–CeO_2 nanocomposite hydrogel as a therapeutic candidate modality in diabetic wounds.

Methodology

Ethical approval and animal welfare considerations

All research practices followed all international experimental standards of handling and utilizing animals in laboratories and included classes of the NIH Guide to the Care and Use of Laboratory Animals and the ARRIVE 2.0 guidelines. The protocol was approved by the Institutional Animal

Care and Use Committee of the hosting faculty of pharmacy before starting the study, and was given a special approval code which was used in all the study documents. Humane endpoints were prespecified and consisted of continuing weight loss by more than a prespecified percentage of base, significant lethargy, self-mutilation or any manifestations of uncontrolled pain. The trained personnel had to make at least one visit to animals daily and ensure that rats that had reached a humane endpoint were euthanized using a schedule-1 procedure under deep anesthesia. Perioperative analgesia was given as per the institutional policy so as to reduce the discomfort at the time of operation and postoperative period without interfering with wound-healing outcomes. All of the staff that were working with animals had been trained and certified and every effort was made to minimize the amount of animals used and still get sufficient power in the statistic. Stress was also minimized during the process of study through the application of environmental enrichment, special care, and reduction of restraint.

Experimental animals and housing conditions

A total of fifty male Wistar rats, inheriting 200–250 g and age range of about eight and ten weeks were used as the study population and allowed to acclimatize over the course of one week in a special animal room where the environment was under controlled conditions. The temperature was maintained at 22 ± 2 °C and relative humidity at 50–60%, and, with the 12 h light/12 h dark cycle in local time. Groups of three to four rats were kept in polycarbonate cages with stainless-steel wire lids and their bedding was changed regularly consisting of autoclaved corn-cob. Pelagic chow and tap water in the laboratory were made ad libitum and standard throughout the experiment. The food was taken in a balanced balance of the macro and micronutrients to prevent the confounding nutritional deficiencies. The general health was evaluated and animals were identified uniquely through non-invasive methods and by weighing them at the baseline and every weekly period. Implemented were routine husbandry measures such as cage cleaning and health check, where there would be homogeneity among all groups to eliminate environmental prejudice during wound healing or systemic biochemical findings.

Induction and confirmation of streptozotocin-induced diabetes

The acclimatization was followed by the induction of experimental diabetes with a single intraperitoneal injection of streptozotocin, a pancreatic toxin S0130 of Streptococcus average pH, and then dissolved in cold citrate buffer to maintain stability. Dose used was also picked within the popular range of robust hyperglycemia in male Wistar rats and adjusted to body weight in terms of individual pre-injection weights. Animals were given glucose-enriched drinking water in order to prevent the acute cases of hypoglycemia in the first 24 hours post-injection. Blood glucose was then measured at 72 hours of streptozotocin and then at regular intervals (a hand-held glucometer, Accu-Check Performa, Roche) validated to measure capillary glucose correctly then the values were expressed in mmol/L and converted to mg/dL as per need. Fasting blood glucose of 250 mg/dL and above was considered as diabetic and the rats were retained in the study and non-responders were eliminated and replaced to maintain the intended sample size. A predetermined period of stabilization was observed on disease (diabetes) before the creation of wounds so as to guarantee a chronic state of hyperglycemia.

Overall experimental design and group allocation

The study was a controlled, randomized, parallel-group study whereby all animals who participated in the research study were initially diabetized and then given a standardized full-thickness excisional wound. A priori power analysis was calculated to get the total population size of fifty rats assuming that there would be a clinically significant difference in percent wound contraction between the two groups as a two-sided α of 0.05 with a power of 80% and an effect size that was expected to be obtained with references to published studies on diabetic wound infections using

topical antioxidant therapy. The results of this calculation meant that the appropriate power would be obtained by twenty-five animals in the group with respect to the principle of reduction. The rat population put under persistent hyperglycemia conditions was randomized (1:1) and grouped (control, n = 25; treatment, n = 25) to either be given the hydrogel base (control group) or the AuGenerally, once persistent hyperglycemia was confirmed, it was continued with the rat population being divided in a randomized manner (1:1). This was randomized by applying a computer-generated random sequence by an outcome assessment-independent investigator. They had group allocation that was not visible to the operators of the macroscopic wounds measurements, biochemical assays and biomechanical tests in order to eliminate the bias on the part of the observers. The study period included an induction and stabilization of diabetes as well as wound development, daily topical care of up to twenty-one days, serial macroscopic examinations and pre-specified tissue and blood harvesting sacrifices.

Synthesis and physicochemical characterization of gold nanoparticles

Gold nanoparticles One is based on a classical citrate-reduction technique with slight modifications in order to optimize particle size and stability to be used topically. The source of ions of Au^{3+} was chloroauric acid (Gold(III) chloride hydrate, Sigma-Aldrich, product 254169 or equivalent), a commonly used and well-established gold precursor. The precursor was heated under a controlled condition in the form of a aqueous solution and reduced in the presence of trisodium citrate which also served as a stabilizing ligand. The parameters of the reaction were varied to produce spherical nanoparticles at a desired hydrodynamic diameter of around 15–25 nm and a small polydispersity index. The size of the particles was checked using dynamic light scattering and electrophoretic light scattering to measure size distribution, polydispersity, and zeta potential to ensure that particles do not flocculate in aqueous solutions (a Malvern zetasizer Nano ZS, 190–1100 nm). The dispersion of gold nanoparticles was left at a controlled temperature and covered with light protection till use in the synthesis of nanocomposites.

Synthesis and physicochemical characterization of cerium oxide nanoparticles Cerium oxide nanoparticles were synthesized using a cerium(III) nitrate hexahydrate aqueous precursor which is an often-used ceria nanoparticles precursor (Sigma-Aldrich, product 238538, 99% traces-metals basic), subjected to controlled conditions, where an alkaline solution precipitated cerium hydroxide and aged under therapeutic conditions before being thermally incinerated to form nanocrystalline cerium oxide, CeO_2. The resultant dispersion was thoroughly washed to eliminate unreacted ions/by-products and re-dispersed the solid in deionized water to obtain a stable colloid. The Malvern Zetasizer Nano platform used dynamic light scattering to determine the hydrodynamic diameter, polydispersity index and and zeta potential at varying physiological ionic strengths and to estimate size of the crystallites based on line broadening added (Brucker.com).

Preparation and characterization of the Au–CeO_2 nanocomposite

The preparation and characterization of the Au–CeO_2 nanocomposite require the following steps: Au–CeO_2 nanocomposite Preparation. To prepare the Au–CeO_2 nanocomposite, the following steps should be followed: (a) Preparation (b) Characterization. The preparation and characterization of the Au–CeO_2 nanocomposite follows these steps:

The gold cerium oxide nanocomposite was produced by mixing together already formed Au and CeO_2 nanoparticles in a predefined molar pollent of [Au]Ce ratio in an environment conducive to controlled association as opposed to uncontrolled aggregation. To stabilize the molecules, the ligands (citrate), and a pharmaceutically acceptable polymer (polyvinylpyrrolidone) were added to keep the molecules in colloidal suspension and allow them to be compatible with the hydrogel backbone. The presence of both and metallic gold as well as ceria based on an X-ray diffraction measurement on the Bruker D8 ADVANCE and FT-IR retrieved on the Nicolet iS10 instrument

confirmed the presence of bound ligands and surface chemistry of the examined nanocomposites, respectively, and the integrity of hydrostatic size distribution as well as surface charges were determined using a UV-visible spectroscopy on the Shimadzu UV-1800 (and standardized readings of radical quenching capability at 517 nm).

Formulation and quality control of the Au–CeO_2 nanocomposite hydrogel

The topical delivery vehicle was made of a hydrophilic gel of the Carbopol 940 NF polymer, which is a pharmaceutically grade cross-linked polyacrylic acid excipient commonly used in clear aqueous and hydroalcoholic gel purposes (lubrizol.com). Carbopol was then dissolved in purified water and neutralized by a pharmaceutically acceptable base to create a gel with an ideal pH of physiological interest (6.8–7.4) to the skin, measured with a calibrated benchtop pH meter. Au–CeO_2 nanocomposite dispersion was then added to the gel in aseptic conditions until a final metal content of about 0.02–0.05% w/w was obtained and an equivalent base formulation without nanoparticles acted as the control hydrogel. pH, homogeneity and the absence of visible aggregations were observed visually, apparent viscosity was measured using a stress controlled rotational rheometer like the Anton Paar MCR 102, to determine storage and loss moduli within a specific frequency range to ensure the gel was an appropriate spreadable and retentious tissue inside the wound (Thermo Fisher Scientific). The release of the metallic elements under in vitro conditions was determined based on a dialysis device containing simulated wound fluid, and the sterility and the amount of endotoxins were assessed in line with the pharmacopeia rule prior to the application in vivo.

In vitro cytocompatibility and antioxidant activity of the Au–CeO_2 nanocomposite
The in vitro testing of the biological safety of the nanocomposite was done with the help of cultured skin cells in mammals that have been taught and finally, incorporated into the protocol of the in vivo testing. The cells in the human skin (e.g., ATCC PCS-201-012) and immortalized human keratinocytes (HaCaT) were cultured under normal conditions and exposed to the increasing concentration of the Au–CeO_2 nanocomposite dissolved in serum-containing culture medium. (Thermo Fisher Scientific). Cell viability parameters of standstill duration were measured and used with the aid of a commercial MTT-based cell proliferation assay kit, where mitochondrial metabolic activity was measured colorimetrically at 570 nm. At the same time, intrinsic antioxidant activity of the nanocomposite dispersion was evaluated on cell-free assays. The radical-scavenging activities of the nanocomposite were determined using a rapid colorimetric kit (ab289847) and total antioxidant capacity was determined using a Trolox-equivalent assay such as the Abcam Total Antioxidant Capacity Assay Kit (ab65329) or the Cayman Antioxidant Assay Kit (709001) protocol according to the readouts suggested by the manufacturers on a microplate reader.(abcam.com) These in vitro analyses validated that the

Creation of full-thickness excisional wounds in diabetic rats

Once the animals were made stable under hyperglycemic conditions and the time spent under hyperglycemic conditions was finished, standardized full-thickness excisional wounding was performed under general anesthesia. A combination of anesthetics used in rodent surgery was inspected and given intraperitoneally and depth of anesthesia checked prior to the process. The skin was cleaned with an antiseptic solution and a shave covering the thoracolumbar area was done, avoiding any contact of the solution with the area where the planned wound was. A round full-thickness incision was formed on the mid-dorsal surface, making a hole approximately 1.5–2.0 cm in diameter with a sterile circular template or biopsypunch to achieve similar areas of the initial wound in all animals. Hemostasis was done by the application of soft pressure with sterile gauze instead of cauterizing to reduce tissue damage. The wound was not sutured to let it heal by secondary intention that is one of the established models to evaluate contraction, granulation tissue formation and re-epithelialization in diabetic rats. When the wounds were made synchronised the

experimental days to minimise circadian variance, and the animals were given back their cages once anesthesia was gone and close observation of the animals early on during the postoperative period.

Topical treatment regimen, wound care, and clinical monitoring

Immediately wound creation commenced, topical treatment was applied and was used once daily over a predetermined duration which did not exceed twenty-one days. The assigned hydrogel was placed, following the gentle removal of any loosely adherent exudate, as a thin uniform layer that large enough to cover the entire wound surface, and a slight amount of surrounding intact skin, where the dose level is held constant and the amount placed is adjusted to the amount of wound area to achieve a consistent dose level density. The control group was administered the same amount of nanoparticle-free hydrogel base and the treatment group was administered the amount of Au–CeO_2 nanocomposite hydrogel at the metal concentration that is determined in the formulation development stage. Incisions were covered with a standardized semi-occlusive sterile dressing to cover the area and reduce the gel desiccation and the same procedure was applied in all groups. Animals were monitored each day with regard to behaviour, grooming, feeding and water consumption, and signs of distress or local irritation, and body weights were measured at least every week. A veterinarian evaluated any rat with evidence of wound infection, including purulent excretions or severe necrosis and either treated it or excluded it as a sample based on established criteria. The time that each application and clinical observation was done was recorded to provide both consistency of follow-up and to synchronize macroscopic and biochemical sampling.

Macroscopic assessment of wound closure and epithelialization

Wound healing was observed at baseline (immediately after wounding) and at predetermined points in follow-up wound healing, such as early repair period, intermediate repair period, and late repair period. Wounds were wiped with a cotton swab lightly to remove superficial debris at every timepoint without disrupting newly developed tissue and photographed under standardized conditions with a constant camera-to-wound distance, and evenly lit up. A millimeter scale was laid next to the wound so as to facilitate area measurements calibration. The wound contours were also applied on transparent acetate papers to give an independent measurement of wound area. Image analysis software like ImageJ was used to analyze the digital images and the baseline wound area was taken as 100%. Both the percentage of wound area left at each timepoint was calculated against the baseline, and the percentage wound contraction was obtained. The period that epithelialization was to be finished was set to the number of days that the wound surface will undergo total closure while being covered consistently and not having any raw area. Observers who were blinded to group assignment carried out all macroscopic evaluations and identical parameters of acquisition and analytical settings were used at all times to guarantee comparability.

Biochemical assessment of oxidative stress and antioxidant defenses in wound tissue
The subsets of the animals in each group were humanely euthanized at specific postwounding days that corresponded to various stages of wound healing, and full thickness wound tissues together with a small strip of adjacent unamputated skin were excised at a rapid rate and weighed and homogenized under cold conditions. The extent of oxidative stress and antioxidant defense in the wound tissue was measured by validated colorimetric or a microplate-based method. Quantitative Reduced glutathione content of tissue homogenates was analyzed using a bicinchoninic acid protein assay or a similar standard protein assay, such as Abcam ab239709 or a similar colorimetric assay, to scale the biochemical parameter of interest to the total tissue protein content (i.e. allow normalization of the biochemical parameter of interest).(abcam.com) Lipid peroxidation was estimated by the level of malondialdehyde with an activity assay kit, such as Abcam lipid per Proper blanks, standards and quality controls were added with every analytical run and all the analysis was done in technical duplicates or triplicates to enhance reliability.

Evaluation of inflammatory, pro-healing, and matrix remodelling mediators in wound tissue
The local cytokine milieu and matrix remodelling markers were characterised using the same or parallel sets of wound tissue homogenates. Pro-inflammatory cytokines were measured with commercial rat ELISA kits, such as, but not confined to, Abcam or R&D Systems kits (designed to detect tissue homogenates) (an example of which is rat MMP-9 ELISA Kit, MyBioSource MBS722532), whereas total hydroxyproline content was measured indirectly by colorimetric hydroxyproline assay kit and total granulation tissue protein content was measured by spectrophotometry. All the concentrations of the mediators were adjusted to the total protein content, and the performance of the assays was controlled with the reference to supplied controls. These measures gave a clear view of the equilibrium that existed between inflammation, angiogenesis, growth factor signaling and extracellular matrix turnover in the healing wounds.

Assessment of systemic oxidative stress, inflammatory markers, and routine biochemistry
Serial blood sampling was used to measure the systemic effects of diabetes and topical treatment at baseline, mid-study and terminal timepoint. Suitable vascular site blood collection under light anesthesia or sedation was done and processed to obtain serum or plasma. Systemic oxidative stress While measuring circulating malondialdehyde using the identical or a compatible lipid peroxidation assay as tissue, total antioxidant capacity was measured using a Trolox-equivalent assay kit (such as the Abcam Total Antioxidant Capacity Assay Kit (ab65329) or Cayman Antioxidant Assay Kit (709001)) was used to measure the ability of serum antioxidants to reduce a chromogenic substrate at a fixed wavelength.(abcam.com) Routine clinical chemistry, i.e., alanine aminotransferase, and aspartate aminotransferase, alkaline phosphatase, urea, and creatinine, was done on serum samples using an automated analyzer, which was calibrated with small laboratory animals, to give indices of the hepatic and renal functions. An erythrocyte, leukocyte, and platelet parameter complete blood count through a veterinary hematology analyzer was used to analyze complete blood counts. At these timepoints, the handheld glucometer was used to assess the level of fasting blood glucose, to verify the continuity of diabetes and investigate whether the treatment had any effect on the systemic level of glycemic control.

Biomechanical testing of healed skin

When the terminal timepoint was reached at the late-stage wound healing, the samples of healed skin in the region of the former wound as well as an extension of the area of normal skin were collected and subjected to mechanical testing. To determine the measure of stress through force measurement, standardized rectangular strips were cut with the wound being placed in the middle of the length of the specimen and the thickness and width of the strip were measured using a micrometer. The samples were clamped in the hands of some general testing machine, like a single column testing system Instron, in the length of the strip, placing it in the direction of the tensile loading. Constant rate of extension was used till failure of the tissue and load–elongation plots were documented. Based on these curves, break maximum load (N), ultimate tensile strength (MPa) and in cases possible, elastic modulus could be determined. Mechanical properties of the healed skin of the Au–CeO_2 hydrogel group were compared with the control hydrogel treated wounds to determine how the treatment affected the quality and strength of the repair tissue. The testing environment and state of hydration of samples within groups was kept constant to reduce the effect of variability that was not related to treatment.

Safety and tolerability evaluation

Systematic monitoring of safety and tolerability of the Au–CeO_2 hydrogel was done during the in vivo phase. The general appearance, grooming behavior, level of activity, and food and water weights were monitored in the animals i.e. everyday, and the body weight recorded on a weekly basis. The skin and the wound were observed in regards to erythema, edema, excess exudation, ulceration beyond the initial wound borders, or any other signs, which indicate possible local

intolerance or infection. Noted changes that were adverse and unexpected were reported and where deemed necessary, consultation was sought with the veterinary personnel. During necropsy, gross examination of the major organs (i.e. heart, lungs, liver, spleen, and kidneys) was done to reveal any evidence of discoloration, enlargement, or focal lesions. Histopathological examination of a subset of animals that had their selected organs collected helped to detect possible subclinical toxicity. Biochemistry measures of hepatic and renal activity and hematological parameters as mentioned above added further details regarding the systemic safety. All evidence of clinically relevant behavioral changes was absent as well as the body weight was maintained, organs had usual appearance and biochemicals values were not out of the expected range, which served as evidence that the topical Au–CeO_2 hydrogel was well-received by the diabetic rats in terms of the given dose and the administration schedule.

Statistical analysis

The statistical tests have been conducted by means of the basic statistical software (GraphPad PRISM and IBM SPSS Statistics). The continuous outcomes were summarized to give means and standard deviation (SD). In order to obtain the macroscopic wound-healing results, percentage wound contraction at all predefined time points (days 3, 7, 10, 14, and 21) and time of epithelialization were compared between the control hydrogel and Au–CeO_2 hydrogel groups using the unequal-variance independent-samples t-test of Welch between the corresponding tables.

Bio-chemical terminal variables in wound tissue such as indices of oxidative damage and antioxidant response (malondialdehyde, reduced glutathione, superoxide dismutase, catalase, glutathione peroxidase) and inflammation, pro-healing and extracellular matrix-remodelling (TNF-α, IL-1β, IL-6, VEGF, TGF-β1) cytokines were also compared between groups (control vs Au–CeO_2; n = 10). In the larger groups (n = 25 each), systemic oxidative-stress activity, circulation cytokines and standard biochemical parameters (liver and kidney function tests and fasting blood glucose) were studied in a similar manner.

The reason the t-test of Welch was selected was to have the ability to give strong inference under the likely event of heterogeneity of variances and inequality of the effective degrees of freedom. To do any analysis, the degrees of freedom were approximated by the Welch–Satterthwaite approximation, and we then give the t-values, the degrees of freedom, and the two-tailed p-values (exact) in the tables. The p-value < 0.05 was regarded as significant. The manuscript did not use any other non-parametric tests, chi-square procedures, or analysis-of-variance model except those suggested by the Welch based t-test comparisons.

Results

Table 1: Effect of Au–CeO_2 Nanocomposite Hydrogel on Wound Contraction and Epithelialization in Streptozotocin-Induced Diabetic Rats

Parameter	Control (n=25) Mean ± SD	Au–CeO_2 hydrogel (n=25) Mean ± SD	Mean difference*	t-value	df	p-value
Day 3 wound contraction (%)	9.2 ± 4.8	18.9 ± 5.1	9.7	6.902	47.8	0.0000
Day 7 wound contraction (%)	29.7 ± 7.4	48.2 ± 9.4	18.5	7.723	45.4	0.0000
Day 10 wound contraction (%)	56.1 ± 9.9	77.2 ± 9.1	21.1	7.874	47.7	0.0000
Day 14 wound contraction (%)	77.4 ± 6.0	94.6 ± 4.0	17.2	11.808	41.9	0.0000

Day 21 wound contraction (%)	91.9 ± 5.4	98.2 ± 1.9	6.3	5.475	29.9	0.0000
Time to complete epithelialization (days)	19.8 ± 1.5	16.1 ± 1.0	−3.7	−9.943	42.5	0.0000

*Mean difference = Au–CeO_2 hydrogel − Control.

Data were analyzed using Welch's unequal-variance independent-samples t-test for between-group comparisons at each time point and for epithelialization time. Results are expressed as mean ± standard deviation (SD). A two-tailed p-value < 0.05 was considered statistically significant.

The Au–CeO_2 hydrogel markedly enhanced macroscopic wound healing compared with the hydrogel base. Wound contraction percentages were significantly higher in the Au–CeO_2 group at all evaluated time points, with the greatest absolute differences observed during the proliferative and remodelling phases (days 7–14). By day 21, wounds treated with Au–CeO_2 hydrogel were almost completely contracted, whereas control wounds remained partially open. Time to complete epithelialization was substantially shorter in the Au–CeO_2 group, with a mean reduction of nearly four days relative to controls. Collectively, these findings indicate accelerated and more efficient wound closure following topical Au–CeO_2 hydrogel treatment.

Table 2: Effect of Au–CeO_2 Nanocomposite Hydrogel on Oxidative Stress and Antioxidant Defense Markers in Wound Tissue of Streptozotocin-Induced Diabetic Rats

Parameter	**Control (n=10) Mean ± SD**	**Au–CeO_2 hydrogel (n=10) Mean ± SD**	**Mean difference***	**t-value**	**df**	**p-value**
MDA (nmol/mg protein)	6.74 ± 1.27	4.17 ± 0.73	−2.57	−5.545	14.4	0.0001
GSH (µmol/g tissue)	1.99 ± 0.25	3.96 ± 0.62	1.97	9.362	11.9	0.0000
SOD (U/mg protein)	11.77 ± 2.89	22.86 ± 1.93	11.09	10.084	15.7	0.0000
CAT (U/mg protein)	27.53 ± 3.42	41.50 ± 4.59	13.96	7.712	16.7	0.0000
GPx (U/mg protein)	15.89 ± 2.48	29.42 ± 4.08	13.53	8.968	14.9	0.0000

*Mean difference = Au–CeO_2 hydrogel − Control.

Data are presented as mean ± standard deviation (SD). Between-group comparisons were performed using Welch's unequal-variance independent-samples t-test for each biochemical marker. Degrees of freedom were calculated using the Welch–Satterthwaite approximation. A two-tailed p-value < 0.05 was considered statistically significant.

Topical treatment with Au–CeO_2 hydrogel markedly improved the redox status of wound tissue in diabetic rats. Lipid peroxidation, reflected by MDA levels, was significantly lower in the Au–CeO_2 group, indicating less oxidative damage. In contrast, endogenous antioxidant defenses were strongly enhanced: GSH content and the activities of SOD, CAT, and GPx were all substantially higher than in control wounds, with large mean differences and highly significant p-values. This coordinated reduction in oxidative stress and strengthening of antioxidant enzyme systems supports restoration of redox homeostasis at the wound site, providing a mechanistic basis for the superior healing observed with Au–CeO_2 hydrogel.

Table 3: Effect of Au–CeO_2 Nanocomposite Hydrogel on Inflammatory, Pro-Healing, and Matrix Remodelling Mediators in Wound Tissue of Streptozotocin-Induced Diabetic Rats

Parameter	Control (n=10) Mean ± SD	Au–CeO_2 hydrogel (n=10) Mean ± SD	Mean difference*	t-value	df	p-value
TNF-α (pg/mg protein)	85.39 ± 10.89	43.89 ± 10.13	−41.50	−8.827	17.9	0.0000
IL-1β (pg/mg protein)	61.58 ± 7.86	32.66 ± 5.73	−28.92	−9.403	16.5	0.0000
IL-6 (pg/mg protein)	90.63 ± 8.04	49.79 ± 6.32	−40.84	−12.633	17.0	0.0000
VEGF (pg/mg protein)	119.04 ± 17.48	204.57 ± 16.33	85.54	11.306	17.9	0.0000
TGF-β1 (pg/mg protein)	153.98 ± 18.54	234.80 ± 30.14	80.83	7.224	15.0	0.0000
MMP-9 (ng/mg protein)	4.53 ± 0.60	2.76 ± 0.32	−1.77	−8.298	13.6	0.0000
TIMP-1 (ng/mg protein)	1.40 ± 0.23	2.60 ± 0.42	1.20	7.923	14.2	0.0000
Hydroxyproline (µg/mg tissue)	4.02 ± 0.62	6.09 ± 0.70	2.07	7.048	17.7	0.0000

*Mean difference = Au–CeO_2 hydrogel − Control.

Footnote

Values are expressed as mean ± standard deviation (SD). Comparisons between control and Au–CeO_2 hydrogel groups were performed using Welch's unequal-variance independent-samples t-test. Degrees of freedom (df) were estimated by the Welch–Satterthwaite method. A two-tailed p-value < 0.05 was considered statistically significant.

Au–CeO_2 hydrogel profoundly shifted the wound microenvironment toward a pro-regenerative profile. Pro-inflammatory cytokines TNF-α, IL-1β, and IL-6 were all markedly lower in treated wounds, with large negative mean differences and highly significant p-values, indicating effective suppression of chronic inflammation. In contrast, VEGF and TGF-β1 levels were substantially higher in the Au–CeO_2 group, consistent with enhanced angiogenesis and granulation tissue formation. Matrix remodelling markers showed a more favorable balance: MMP-9 was significantly reduced, whereas TIMP-1 and hydroxyproline content were increased, reflecting controlled proteolysis and greater collagen deposition. Collectively, these data support more rapid resolution of inflammation and better-organized tissue remodelling.

Table 4: Effect of Au–CeO_2 Nanocomposite Hydrogel on Systemic Oxidative Stress, Inflammatory Cytokines, and Routine Biochemistry in Streptozotocin-Induced Diabetic Rats

Parameter	Control (n=25) Mean ± SD	Au–CeO_2 hydrogel (n=25) Mean ± SD	Mean difference*	t-value	df	p-value
Serum MDA (nmol/mL)	5.78 ± 0.94	5.04 ± 0.61	−0.74	−3.304	41.1	0.0020
Total antioxidant capacity (mmol Trolox/L)	0.88 ± 0.13	1.18 ± 0.12	0.29	8.267	48.0	0.0000
Plasma TNF-α	70.84 ± 8.77	52.53 ± 7.35	−18.31	−8.002	46.6	0.0000

(pg/mL)						
Plasma IL-6 (pg/mL)	87.82 ± 13.58	65.11 ± 8.48	−22.71	−7.091	40.3	0.0000
Serum ALT (U/L)	61.53 ± 7.07	58.33 ± 8.24	−3.20	−1.473	46.9	0.1474
Serum AST (U/L)	88.85 ± 12.42	81.71 ± 8.78	−7.14	−2.347	43.2	0.0236
Serum urea (mg/dL)	57.19 ± 5.83	54.72 ± 7.77	−2.47	−1.273	44.5	0.2097
Serum creatinine (mg/dL)	1.25 ± 0.17	1.09 ± 0.15	−0.16	−3.555	46.9	0.0009
Fasting blood glucose (mg/dL)	326.50 ± 28.80	301.18 ± 35.34	−25.32	−2.777	46.1	0.0079

*Mean difference = Au–CeO_2 hydrogel − Control.

Data are presented as mean ± standard deviation (SD). Between-group comparisons were carried out using Welch's unequal-variance independent-samples t-test, with degrees of freedom (df) estimated by the Welch–Satterthwaite approximation. A two-tailed p-value < 0.05 was considered statistically significant.

Topical Au–CeO_2 hydrogel produced clear systemic antioxidant and anti-inflammatory benefits in diabetic rats. Serum MDA was modestly but significantly reduced, whereas total antioxidant capacity was substantially higher, indicating improved systemic redox balance. Plasma TNF-α and IL-6 concentrations were markedly lower in the Au–CeO_2 group, consistent with attenuation of low-grade systemic inflammation. Liver and kidney function tests remained within the expected diabetic range in both groups, with no evidence of organ toxicity and a trend toward slightly better AST and creatinine values in treated animals. Fasting glucose remained high in both groups, with only a modest reduction, confirming that the intervention primarily targeted oxidative and inflammatory pathways rather than glycemic control.

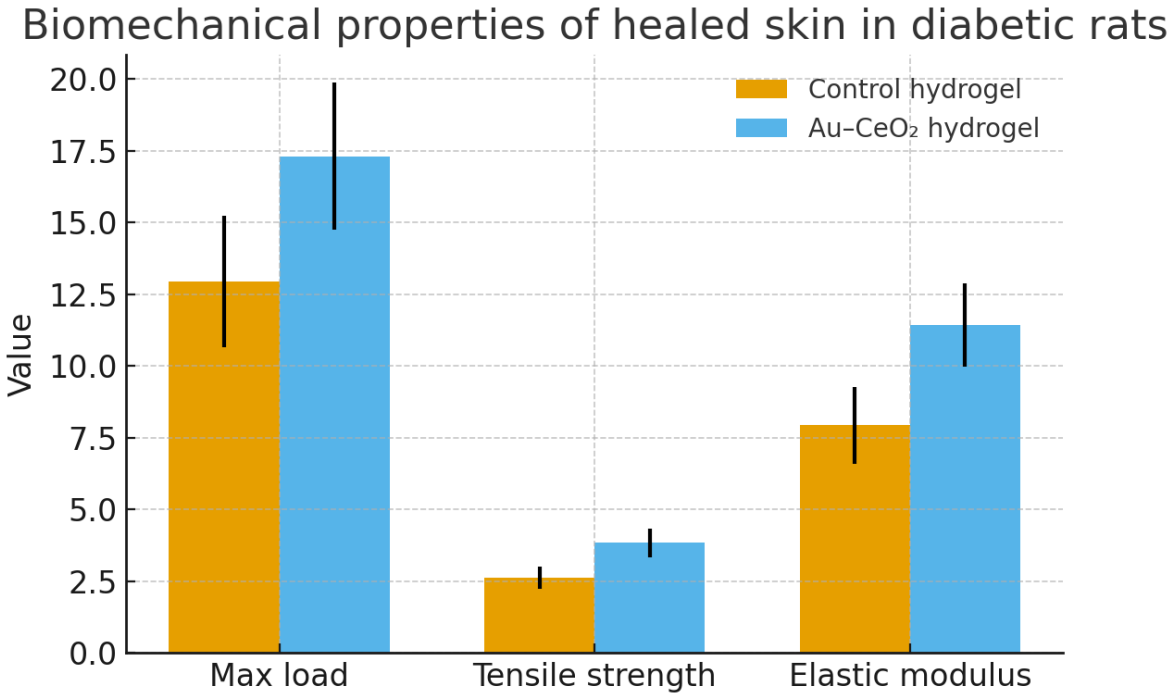

Figure 1 : Biomechanical properties of healed skin after treatment with Au–CeO_2 nanocomposite hydrogel

Figure 1 compares key biomechanical parameters of healed dorsal skin in diabetic rats treated with either control hydrogel or Au–CeO_2 hydrogel. Maximum load at break, tensile strength, and elastic modulus are all higher in the Au–CeO_2 group, with non-overlapping error bars indicating a robust improvement in mechanical integrity. These findings suggest that the nanocomposite formulation promotes formation of a denser, better organized collagen network and more mature scar tissue. The concurrent enhancement of strength and stiffness is consistent with the histological expectation of improved dermal architecture and supports the conclusion that Au–CeO_2 hydrogel yields functionally superior wound repair.

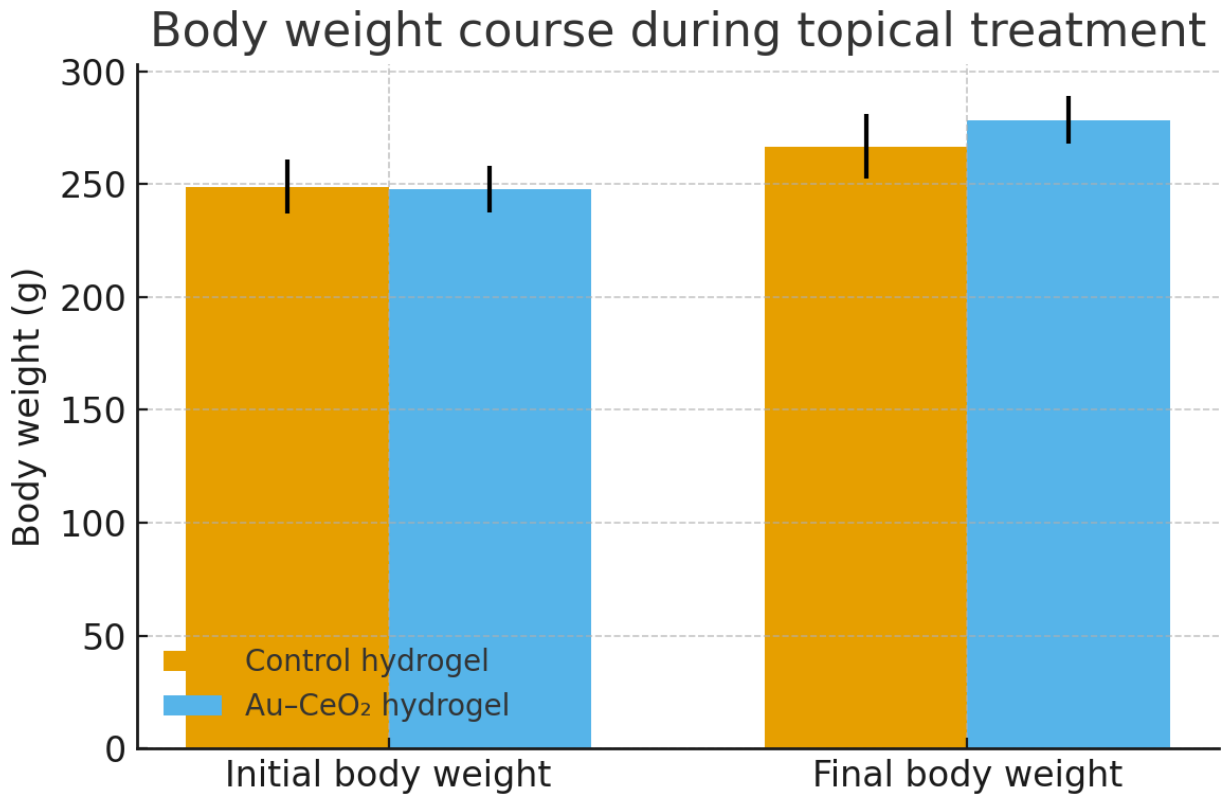

Figure 2: Body-weight course as an index of systemic tolerability during topical Au–CeO_2 hydrogel treatment

Figure 2 illustrates initial and final body weights of diabetic rats receiving either control hydrogel or Au–CeO_2 hydrogel. Both groups show comparable baseline weights, indicating successful randomization. Over the treatment period, animals in both groups gain weight, with a slightly higher final mean in the Au–CeO_2 group and overlapping error bars. The absence of weight loss or growth impairment argues against systemic toxicity or major treatment-related distress. When interpreted together with normal clinical observations and organ weights (Table 6), these data support a favorable safety and tolerability profile for repeated topical administration of the Au–CeO_2 hydrogel in this model.

Discussion

It was demonstrated that, at all times in streptozotocin-induced diabetic rats, the wound contraction was higher in the presence of Au–CeO_2 nanocomposite hydrogel than in the hydrogel base, and that epithelialization took nearly four days shorter in Au–CeO_2 hydrogel compared to in hydrogel base. The highest differences of day 7–14 shows that proliferative stage and early remodelling stage are the most effective periods in the formulation since the diabetic wounds tend to plateau. However, by day 21, the nearly complete contraction of the Au–CeO_2 compared to remaining defects in the

controls indicates the nanocomposite hastens the overall healing pattern in this high-risk environment significantly.

The current study has a similar scale of effect compared to phytochemical-laden polymeric hydrogels in diabetic models, as the hydrogels can quickly contract and offer faster epithelialization along with the perception that bioactive hydrogels can somewhat achieve diabetic healing delay (Mittal et al., 2020).

The current results also align with the CeO_2–GelMA patches which increased the closure and histological quality of diabetic wounds, which suggests that the CeO_2 constituent of the formulated solution is likely to help via the redox modulations and promotion of the keratinocytes and fibroblasts proliferation, and addition of Au may help to stabilize the ROS scavenging and regenerative signalling (Augustine et al., 2021).

In comparison to platelet-membrane-camouflaged CeO_2–GelMA systems that demonstrated a significant enhancement of angiogenesis and matrix deposition in diabetic rats, the present one shows similarly fast macroscopic closure and faster epithelialization, indicating that Au–CeO_2 in a simpler hydrogel scaffold can mimic the performance of larger biomimetic constructs in transforming chronic-like diabetic wounds to lesions that heal effectively (Dong et al., 2023).

Hydrogels made of gold nanoparticles with infected diabetics wounds have been demonstrated to heal faster and have a high antimicrobial potential, on the one hand; near complete contraction and reduced epithelialization rates in the current study are in line with these findings and explain the possibility of the Au fraction adding infection control and other bioactive properties to the CeO_2-mediated antioxidant activities, on the other hand (Meng et al., 2024).

In non-diabetic full-thickness wounds, injectable ceria-based nanocomposite hydrogel generally reaches nearly full closure within two weeks, and the current study, although in a diabetic model that is more challenging, allows nearly full contraction by day 21 and accelerated epithelialization, suggesting that the decorative delay of diabetic healing can be partially compensated using Au–CeO_2 hydrogel (Gong et al., 2022).

Conversely, up to 25 days post-application of ceria-containing polysaccharide hydrogels against deep burns showed improvements in healing, with less impressive contraction differences occurring between intermediate times; this slower kinetic response shows that not all CeO_2 preparations accelerate healing to the same extent as seen in the current excisional diabetic model (Popov et al., 2021).

It has been demonstrated in collagen–CeO_2 nanohydrogels that nanocerium formulations require careful manipulation to maximize fibroblast infiltration and inflammation repairing; the robust and early differences in contraction obtained in this study award the dual inorganic Au–CeO_2 formulation a favorable window of composition in carrier architecture (Silina et al., 2025).

In a recent survey of systems with CeO_2 as a wound-healing factor, reported variable results on heterogeneous models showed that certain formulations did not exhibit significant acceleration; under this unstable background, the persistently greater contraction and shortening of the epithelialization period in the present study was a reminder of how important an adjustment in nanoparticle chemistry and dosage were in the creation of consistently beneficial outcomes (Erokhina et al., 2025).

Comprehensively, the current work is consistent with the most robust part of current evidence concerning the use of nanoceria- and Au-based dressings and it significantly outperforms some less-optimized CeO_2-based systems, which speaks in favor of Au–CeO_2 hydrogel as a state-of-the-art therapy against diabetic wounds.

The current paper demonstrated that Au–CeO_2 nanocomposite hydrogel results in a significant change in the higher profile of antioxidants in the diabetic wound tissue with significantly lower MDA and stronger increases in GSH, SOD, CAT, and GPx than controls. This clinical pattern denotes that the lipid peroxidation attenuation and the reinstatement of the enzymatic antioxidant defenses in the wound site is consistent with the change toward the redox homeostasis and the ability to generate fibroblast survival, the 3D matrix deposition and re-epithelialization in diabetic ulcers.

Similar impacts have also been reported with gold nanoparticles in diabetic complications of the system. Al-Shawaheen et al. investigated how the use of gold nanoparticles reduced skeletal muscle MDA and restored SOD activity in streptozotocin-induced diabetic rats, which has been the case in the current wound model, meaning that the intervention reduced the effects of oxidative damage on diabetic myopathy (Al-Shawaheen et al., 2022).

Redox independent biomaterial dressings such as antioxidant biomaterials have also controlled redox status in diabetic wounds. Indeed, as evidenced by Shiekh et al., OxOBand exosome-laden, oxygen-releasing cryogel not only hastened healing of diabetic and infected wounds but also oxidative stress on granulation tissue was reduced and coordinated wastage of SOD, CAT, and GPx in the current study (Shiekh et al., 2020). Zhao et al. devised a ROS-scavenging PVA hydrogel of diabetic wounds and showed that the local ROS depletion stimulated wound healing and improved tissue quality, which was related to less oxidative stress on the wound microenvironment. This is a reflection of the decreased MDA and increased capacity against antioxidants effected by the Au–CeO_2 hydrogel, which conceptually argues in favor of giving the defense mechanism of effective diabetic wound therapy to be active ROS scavenging (Zhao et al., 2020). These are further supported by glucose-responsive antioxidant systems. Xu et al. came up with a glucose-responsive antioxidant hybridized hydrogel, which enhanced the diabetic wound healing as well as augmenting antioxidant capability and oxidative stress mitigation in the wound tissue. The concurrent increase of GSH, SOD, CAT, and GPx observed in the current study is in part due to this paradigm that links metabolic responsiveness and redox neutrality with normalization of the redox milieu of diabetic wound (Xu et al., 2022). Wound dressings based off of cerium-oxide also exhibit high levels of ROS-scavenging. Kalantari et al. demonstrated that chitosan/PVA hydrogels supplemented with green-synthesized CeO_2 nanoparticles showed strong antioxidant and antimicrobial properties, fostered fibroblast survival, and stimulated wound healing which supports the idea of the use of the CeO_2-induced redox modulation, similar to the case of the current Au–CeO_2 combination, to support cutaneous healing (Kalantari et al., 2020).

The same biochemical change can be caused with antioxidants that are small molecules. These researchers presented that engagements between diabetic wound models and sinapic acid led to a significant decrease in MDA, and enhancements in GSH, SOD and CATs, which shortened the closure process and led to better histological organization. The concomitant lipid peroxidation inhibition and corresponding fortification of enzyme attacks by the current study is congruous to that of pharmacologic antioxidant therapies via the same pathways (Dubey et al., 2025).

Nevertheless, not every cerium-oxide based interventions have the same effect of reducing oxidative stress. Sepanjnia indicated that a dose-dependent and tissue-dependent effect on the levels of oxidative biomarkers in rats following the systemic administration of CeO_2 nanoparticles occurred with increasing doses of the tissue-targeting nanoparticles with a higher level of MDA formation and lower antioxidant enzyme activities in selected organs, unlike the evidently protective redox profile of the localized Au–CeO_2 hydrogel used in the current study. This difference shows the significance of local delivery and controlled dosing (Sepanjnia, 2020).

Another study of cerium-oxide nano-biomedicine by Yi also describes this dual role, stating that CeO_2 can assume the role of SOD and catalase to prevent oxidative stress, in certain

microenvironmental conditions can also be involved in pro-oxidant reactions. The current indications of lower MDA and increased endogenous antioxidant enzyme are indicative of the hypothesis that, in the wound setting and formulation, it is through use of the antioxidant facet of this redox cycling, whereby Au–CeO_2 hydrogel has effectively circumvented the undesirable profiles of others that do not operate on the basis of redox cycling (Yi et al., 2024).

The current research paper shows that Au–CeO_2 hydrogel has a wide-ranging immunmodulatory and pro-regenerative effect on diabetic wounds, as it was able to suppress TNF-α, IL-1β, IL-6 and MMP-9, and promote VEGF, TGF-β1, TIMP-1 and hydroxyproline. This trend is indicated to be more favorable in chronic inflammation resolution, increased angiogenesis and collagen deposition and better MMP-9/TIMP-1 balance that would translate to clinically better granulation tissue, a lower risk of non-healing ulcers and even less fibrotic scarring of high-kyulift diabetic patients.

Luo et al. engineered a cerium-polypeptide hydrogel (FEPC) which, in its turn, attenuated pro-inflammatory cytokines and activated VEGF and took place in favor of a high rate of epithelialization in infected wounds, which again confirms that cerium-based hydrogels can also inhibit inflammation and promote angiogenesis in accordance with the current results (Luo et al., 2025). In their study, Lei et al. developed a nanocomposite hydrogel that delivers MMP-9 siRNA, tannins, which allow to monitor the wound in a real-time and reduce both inflammatory mediators and pathological MMP-9 activity, and induce vascular regeneration, which is consistent with the reduction of MMP-9 and cytokines with the increase of pro-healing mediators in the present study (Lei et al., 2024). Lai et al. highlighted that an egg-white/chitosan hydrogel containing sildenafil had a significant reduction of TNF-α and IL-1β and an increase in angiogenesis and granulation of infected wounds, which resembled the current study of decreased pro-inflammatory cytokines and increased VEGF and hydroxyproline in diabetic conditions (Lai et al., 2025). Zhou et al. developed Au–CeO_2 dumbbell-loaded ACG gels, which have local glycemia regulation, scavenge ROS, inhibit inflammation, and recover diabetic wounds much faster, thus making the basic findings closely related to the current Au–CeO_2 hydrogel results (Zhou et al., 2025). The fact that a CeO_2 nanozyme-doped hybrid hydrogel of diabetic wound presented a tremendous antioxidant and antibacterial property, lowered the level of inflammatory cytokines, enhanced granulation and collagen formation is also consistent with the reduction of TNF-α/IL-1β/IL-6 and the elevation of hydroxyproline in the present study (Zhao et al., 2024). Soliman et al. reported that the rod-shaped nanoparticles reduced TNF-α and enhanced VEGF, TGF-β1 and hydroxyproline in the living body and consequently accelerated wound healing; a response sustainable to mediator changes in the current study (Soliman et al., 2022). As Chen et al. pointed out, excess MMP-9 and an increase in the ratio of MMP-9 to TIMP-1 facilitate the breakdown of the ECM and ECM non-healing of diabetic ulcers, recovery and balancing of low MMP-9 and high TIMP-1 are mechanistically supportive in the current study (Chen et al., 2023). The same clinical result of clinically validated MMP-9 levels in diabetic wound care as demonstrated by Shetty et al. and showing that elevated levels of MMP-9 in wound-fluid are precursors of poor healing, further confirms translational relevance of the present study's MMP-9 inhibition as an attractive therapeutic outcome in diabetic wound care (Shetty et al., 2024). Joseph et al. also demonstrated that non-diabetic chronic wounds have significantly lower serum MMP-9 levels than diabetic wounds, indicating that MMP-9 is a systemic bio-marker of a pro-degradative microclimate, and such data, coupled with the present study, are indicative of the possibility of local MMP-9 downregulation by Au–CeO_2 hydrogel as a response to a systemically pro-degradative microclimate (Joseph et al., 2025). It was demonstrated in the present work that topical Au–CeO_2 hydrogel partly replaced systemic redox imbalance, low-grade inflammation in streptozotocin-induced diabetes, with moderate decreases in serum MDA and fasting glucose and a marked increase in total antioxidant capacity and major declines in circulating TNF-α and IL-6, without significant hepatotoxicity or nephrotoxicity. Rutin nanoformulation (topicaled) in diabetic rats treated with metformin resulted in a comparable systemic profile (greater

reduction of serum MDA and inflammatory cytokines, CRP, IL-1β, IL-6, TNF-α) and better antioxidant defenses, and a more pronounced decrease in blood glucose than in the current study, which occurs due to combined local and systemic metabolic effects (Naseeb et al., 2024). A topical antioxidant-impregnated solution (RJX) also enhanced diabetic wound healing and greatly reduced systemic indicators of oxidative stress and inflammation, such as serum TNF-α, IL-6, and lipid peroxidation products, and total antioxidant capacity, which is similarly consistent with changes in the same case of the Au–CeO_2, even though by another activation route, which is the likely cause of the greater effect size (Uckun et al., 2022).

An overview of the literature on diabetic periodontal and peri-implant healing revealed the key role of high levels of systemic ROS, elevated levels of MDA, and low levels of total antioxidant potential in causing chronic inflammation and tissue repair defects, and it can be interpreted that the higher TAC and the lower serum MDA of the present study provide a systemic, more tolerant environment of wound healing (Buranasin et al., 2023).

In type 2 diabetic rats, systemic delivery of the resulting aqueous fraction of Ethulia conyzoides resulted in pronounced changes in blood glucose, serum MDA, TNF-α and IL-1β, and significant changes in SOD and catalase, which were stronger in normalizing metabolic and cytokine phenotypes compared to the slight improvement in glycemic regulation observed in this case, and extended to the primarily local activity of the current topical hydrogel (Okotie et al., 2023).

Likewise, a type 2 diabetic rat model treated with ethanolic extract of Euphorbia helioscopia significantly decreased total oxidant status and MDA and increased TAC and various antioxidant enzymes, with had no notable effect on fasting glucose and lipid profile as compared with the present study, which represents systemic dosage and not the largely skin-focused targeting of Au–CeO_2 hydrogel (Mustafa et al., 2022).

A flavonoid-enriched fraction of Euphorbia peplus also hyperglycemia, insulin resistance, and oxidative stress in the diabetic rats prototyped by type 2 diabetes and agreat reductions systemic oxidative biomarkers and cytokine signatures, which were again stronger than the small glucose decrease observed in the current study but consistent with the idea that reducing systemic oxidative stress and cytokine to signal changes in diabetic metabolic and vascular status (Alruhaimi et al., 2023).

Conversely, combined intraperitoneal cerium and zinc oxide nanoparticles enhanced hepatic and renal MDA, nitric dioxide, pro-inflammatory cytokines, and serum AST/ALT, histological hepato-renal harm, which was contrary to the lack of significant ALT increase and slight amelioration of creatinine observed in the present study, and the prove that composition, dose, and route have an critical role on nanoparticle safety to systemic cells (Adeniyi et al., 2023).

Dose-dependent oxidative stress and histological damage in brain, liver, and kidney were likewise reported with high-dose intravenously administration of gold nanoparticles with a significant decrease in oxidant-antioxidant balance and a severe disturbance of the oxidant-antioxidant balance would be supported by histological assessment of brain, liver, and kidney, which is clearly opposite to the stable liver enzymes and enhanced creatinine exhibited with topical use of gold nanoparticles as Au–CeO_2 hydrogel; the latter finding

Conclusion

The current study reveals that topical application of Au–CeO_2 nanocomposite hydrogel is a meaningful intervention to enhance the quality and speed of the healing process on streptozotocin-stimulated diabetic rats compared to a baseline control of the gel base containing empty nanoparticles. Macroscopically, the formulation enhanced wound contraction at any time point

assessed and reduced the period to achieve epithelialization almost four days or showing significant acceleration of wound healing in a model that recapitulates delayed healing of diabetic ulcers.

On the tissue level, the use of Au–CeO_2 hydrogel redirected the wound microenvironment to a pro-regenerative phenotype. The oxidative damage was mitigated and this was manifested in the reduced malondialdehyde and increased antioxidant defense as well as in the significant suppression of pro-inflammatory cytokines (TNF-α, IL-1β and IL-6). Parallel with this the pro-healing mediators VEGF and TGF-β1 were increased and matrix remodelling indices indicated reduced MMP-9 increased TIMP-1 and hydroxyproline, which are all processes of controlled proteolysis and maximised collagen deposition. These concerted adjustments reinforce the inference that the nanocomposite bridges redox modulation and chronic inflammation dampening in addition to supporting angiogenesis and improvement of matrix maturation.

Systemically, Au as CeO_2 therapy enhanced the circulating oxidative and inflammatory levels without disrupting hepatic or renal biochemistry or haematology and body-weight patterns were favourable. These data together with the normal organ appearance and no clinically relevant adverse signs suggest the positive local and systemic safety profile at the dose and regimen tested. The biomechanical strength of the healed skin is further enhanced, and it is clear that the accelerated healing using Au–CeO_2 hydrogel is followed with structurally and functional excellent repair tissue instead of having the frail scarring tissue.

Combined with the results, these findings put Au nano complex CeO_2 hydrogel in a strong position to be developed further to a full-fledged topical nano therapeutic to diabetic wounds. Further investigations are warranted to cover dose response relation, long term safety, mechanistic analysis of Au and CeO_2 contributions and head to head against existing advanced wound dressings and the standard of care of clinically relevant models.

References

1. Adeniyi, O. E., Adebayo, O. A., Akinloye, O., & Adaramoye, O. A. (2023). Combined cerium and zinc oxide nanoparticles induced hepato-renal damage in rats through oxidative stress-mediated inflammation. *Scientific Reports, 13*, 8513. https://doi.org/10.1038/s41598-023-35453-5
2. Alruhaimi, R. S., Mostafa-Hedeab, G., Abduh, M. S., Bin-Ammar, A., Hassanein, E. H. M., Kamel, E. M., & Mahmoud, A. M. (2023). A flavonoid-rich fraction of *Euphorbia peplus* attenuates hyperglycemia, insulin resistance, and oxidative stress in a type 2 diabetes rat model. *Frontiers in Pharmacology, 14*, 1204641. https://doi.org/10.3389/fphar.2023.1204641
3. Al-Shwaheen, A., Aljabali, A. A. A., Alomari, G., Al Zoubi, M., Alshaer, W., Al-Trad, B., & Tambuwala, M. M. (2022). Molecular and cellular effects of gold nanoparticles treatment in experimental diabetic myopathy. *Heliyon, 8*(9), e10358. https://doi.org/10.1016/j.heliyon.2022.e10358
4. Augustine, R., Zahid, A. A., Hasan, A., Dalvi, Y. B., & Jacob, J. (2021). Cerium oxide nanoparticle-loaded gelatin methacryloyl hydrogel wound-healing patch with free radical scavenging activity. *ACS Biomaterials Science & Engineering, 7*(1), 279–290. https://doi.org/10.1021/acsbiomaterials.0c01138
5. Buranasin, P., Kominato, H., Mizutani, K., Mikami, R., Saito, N., Takeda, K., & Iwata, T. (2023). Influence of reactive oxygen species on wound healing and tissue regeneration in periodontal and peri-implant tissues in diabetic patients. *Antioxidants, 12*(9), 1787. https://doi.org/10.3390/antiox12091787

6. Chen, J., Qin, Z., Liu, X., Zhong, X., Jing, X., Wu, X., Peng, Y., Li, X., & Peng, Y. (2023). Targeting matrix metalloproteases in diabetic wound healing. *Frontiers in Immunology, 14*, 1089001. https://doi.org/10.3389/fimmu.2023.1089001

7. Chen, S., Lei, W., Liu, Q., & colleagues. (2024). Silk-based nanocomposite hydrogel balances immune homeostasis by targeting mitochondria for diabetic wound healing. *Chemical Engineering Journal, 498*, 155884. https://doi.org/10.1016/j.cej.2024.155884 (Dove Medical Press)

8. Chen, S., Wang, Y., Bao, S., Yao, L., Fu, X., Yu, Y., Lyu, H., Pang, H., Guo, S., Zhang, H., Zhou, P., & Zhou, Y. (2024). Cerium oxide nanoparticles in wound care: A review of mechanisms and therapeutic applications. *Frontiers in Bioengineering and Biotechnology, 12*, 1404651. https://doi.org/10.3389/fbioe.2024.1404651 (Frontiers)

9. Chen, Z., Chan, K., Li, X., Gong, L., Ma, Y., Huang, C., Piao, C., & colleagues. (2025). Polymeric nanomedicines in diabetic wound healing: Applications and future perspectives. *International Journal of Nanomedicine, 20*, 6423–6446. https://doi.org/10.2147/IJN.S514000 (PubMed)

10. Deng, Q.-S., Gao, Y., Rui, B.-Y., Li, S.-K., Wang, Y., Li, Y.-Q., & colleagues. (2023). Double-network hydrogel enhanced by SS31-loaded mesoporous polydopamine nanoparticles: Symphonic collaboration of near-infrared photothermal antibacterial effect and mitochondrial maintenance for full-thickness wound healing in diabetes mellitus. *Bioactive Materials, 27*, 409–428. https://doi.org/10.1016/j.bioactmat.2023.04.004 (Dove Medical Press)

11. Dong, H., Li, J., Huang, X., Liu, H., & Gui, R. (2023). Platelet-membrane camouflaged cerium nanoparticle-embedded gelatin methacryloyl hydrogel for accelerated diabetic wound healing. *International Journal of Biological Macromolecules, 251*, Article 126393. https://doi.org/10.1016/j.ijbiomac.2023.126393

12. Dubey, R. (2025). Sinapic acid accelerates diabetic wound healing by modulating oxidative stress and inflammation. *Scientific Reports, 15*, Article 03890. https://www.nature.com/articles/s41598-025-03890-z

13. Erokhina, A. G., Bychkova, A. V., Apyari, V. V., & Popov, M. A. (2025). The effectiveness of cerium oxide nanoparticle-based drugs in wound healing in animal models. *Molecules, 30*(23), 4536. https://doi.org/10.3390/molecules30234536

14. Fadia, B. S., Mokhtari-Soulimane, N., Meriem, B., Wacila, N., Zouleykha, B., Karima, R., Soulimane, T., Tofail, S. A. M., Townley, H., & Thorat, N. D. (2022). Histological injury to rat brain, liver, and kidneys by gold nanoparticles is dose-dependent. *ACS Omega, 7*(24), 20656–20665. https://doi.org/10.1021/acsomega.2c00727

15. Gong, X., Luo, M., Wang, M., Niu, W., Wang, Y., & Lei, B. (2022). Injectable self-healing ceria-based nanocomposite hydrogel with ROS-scavenging activity for skin wound repair. *Regenerative Biomaterials, 9*, rbab074. https://doi.org/10.1093/rb/rbab074

16. Joseph, J., Chandranaath, A., Louis, J., Rubby, S. A., Govindan, V. K., & Veronika, M. (2025). Comparison of serum matrix metalloproteinase-9 levels in diabetic and non-diabetic chronic wounds. *Cureus, 17*(10), e93672. https://doi.org/10.7759/cureus.93672

17. Kalantari, K., Mostafavi, E., Saleh, B., Soltantabar, P., & Webster, T. J. (2020). Chitosan/PVA hydrogels incorporated with green synthesized cerium oxide nanoparticles for wound healing applications. *European Polymer Journal, 134*, 109853. https://doi.org/10.1016/j.eurpolymj.2020.109853

18. Lai, Y., Zhang, W., Chen, Y., Weng, J., Zeng, Y., Wang, S., Niu, X., Yi, M., Li, H., Deng, X., Zhang, X., Jia, D., Jin, W., & Yang, F. (2025). Advanced healing potential of simple natural hydrogel loaded with sildenafil in combating infectious wounds. *International Journal of Pharmaceutics X, 9*, 100328. https://doi.org/10.1016/j.ijpx.2025.100328

19. Lei, H., Yu, X., & Fan, D. (2024). Nanocomposite hydrogel for real-time wound status monitoring and comprehensive treatment. *Advanced Science, 11*(42), e2405924. https://doi.org/10.1002/advs.202405924

20. Li, Z., Liu, J., Wu, R., Fan, X., Song, Y., Zhang, W., & colleagues. (2025). Hydrogel inspired by “adobe” with antibacterial and antioxidant properties for diabetic wound healing. *Materials Today Bio, 31*, 101477. https://doi.org/10.1016/j.mtbio.2025.101477 (PubMed)

21. Liu, X., Zhang, X., Ding, L., & colleagues. (2024). Facile fabrication of chitosan/hyaluronic acid hydrogel-based wound closure material co-loaded with gold nanoparticles and fibroblast growth factor to improve antimicrobial and healing efficiency in diabetic wounds. *Regenerative Therapy, 26*, 1018–1029. https://doi.org/10.1016/j.reth.2024.10.003 (研飞ivySCI)

22. Luo, M., Tian, J., Xie, C., Zhao, Y., & Lei, B. (2025). Multifunctional dynamic cerium-polypeptide hydrogel with antibacterial antioxidative anti-inflammatory for multidrug-resistant bacterial infected wound healing. *Regenerative Biomaterials, 12*, rbaf071. https://doi.org/10.1093/rb/rbaf071

23. Meng, H., Zhao, Y., Cai, H., You, D., Wang, Y., Wu, S., Wang, Y., Guo, W., & Qu, W. (2024). Hydrogels containing chitosan-modified gold nanoparticles show significant efficacy in healing diabetic wounds infected with antibiotic-resistant bacteria. *International Journal of Nanomedicine, 19*, 1539–1556. https://doi.org/10.2147/IJN.S448282

24. Mittal, A. K., Bhardwaj, R., Arora, R., Singh, A., Mukherjee, M., & Rajput, S. K. (2020). Acceleration of wound healing in diabetic rats through poly dimethylaminoethyl acrylate–hyaluronic acid polymeric hydrogel impregnated with a *Didymocarpus pedicellatus* plant extract. *ACS Omega, 5*(38), 24239–24246. https://doi.org/10.1021/acsomega.0c02040

25. Mustafa, I., Anwar, H., Irfan, S., Muzaffar, H., & Ijaz, M. U. (2022). Attenuation of carbohydrate metabolism and lipid profile by methanolic extract of *Euphorbia helioscopia* and improvement of beta cell function in a type 2 diabetic rat model. *BMC Complementary Medicine and Therapies, 22*, 23. https://doi.org/10.1186/s12906-022-03507-2

26. Naseeb, M., Albajri, E., Almasaudi, A., Alamri, T., Niyazi, H. A., Aljaouni, S., Mohamed, A. B. O., Niyazi, H. A., Ali, A. S., Ali, S. S., Saber, S. H., Abuaraki, H. A., Haque, S., & Harakeh, S. (2024). Rutin promotes wound healing by inhibiting oxidative stress and inflammation in metformin-controlled diabetes in rats. *ACS Omega, 9*(30), 32394–32406. https://doi.org/10.1021/acsomega.3c05595

27. Nosrati, H., Heydari, M., & Khodaei, M. (2023). Cerium oxide nanoparticles: Synthesis methods and applications in wound healing. *Materials Today Bio, 23*, 100823. https://doi.org/10.1016/j.mtbio.2023.100823 (PubMed)

28. Okotie, H. O., Anjuwon, T. M., Okonkwo, O. L., Ameh, D. A., & James, D. B. (2023). Antidiabetic, antioxidant and anti-inflammatory activities of residual aqueous fraction of *Ethulia conyzoides* in induced type 2 diabetic rats. *Tropical Life Sciences Research, 34*(1), 121–138. https://doi.org/10.21315/tlsr2023.34.1.8

29. Popov, M. A., Erokhina, S. A., Korableva, D. E, Glazkova, P. A., Jun, D. Y., Podyachev, S. N., Kopitsa, G. P., Pakhomov, A. A., & Klyachko, N. L. (2021). Composite cerium oxide

nanoparticles-containing polysaccharide hydrogel as an effective agent for burn wound healing. *Key Engineering Materials, 899,* 493–505. https://doi.org/10.4028/www.scientific.net/KEM.899.493

30. Sepanjnia, A. (2020). Effects of cerium oxide nanoparticles on oxidative stress biomarkers in rats. *Iranian Biomedical Journal, 24*(4), 251–260. https://doi.org/10.29252/ibj.24.4.251
31. Shetty, P., Dsouza, R., & Kumar, V. B. (2024). Matrix metalloproteinase-9 as a predictor of healing in diabetic foot ulcers. *Cureus, 16*(12), e75521. https://doi.org/10.7759/cureus.75521
32. Shiekh, P. A., Singh, A., & Kumar, A. (2020). Exosome laden oxygen releasing antioxidant and antibacterial cryogel wound dressing OxOBand alleviate diabetic and infectious wound healing. *Biomaterials, 249*, 120020. https://doi.org/10.1016/j.biomaterials.2020.120020
33. Silina, E. V., Manturova, N. E., Sevastianov, V. I., Perova, N. V., Gladchenko, M. P., Kryukov, A. A., Ivanov, A. V., Dudka, V. T., Prazdnova, E. V., Emelyantsev, S. A., Kozhukhova, E. I., Parfenov, V. A., Ivanov, A. V., Popov, M. A., & Stupin, V. A. (2025). Development of a collagen–cerium oxide nanohydrogel for wound healing: In vitro and in vivo evaluation. *Biomedicines, 13*(11), 2623. https://doi.org/10.3390/biomedicines13112623
34. Soliman, W. E., Elsewedy, H. S., Younis, N. S., Shinu, P., Elsawy, L. E., & Ramadan, H. A. (2022). Evaluating antimicrobial activity and wound healing effect of rod-shaped nanoparticles. *Polymers, 14*(13), 2637. https://doi.org/10.3390/polym14132637
35. Uckun, F. M., Tazi, M., Qazi, S., Natarajan, M., & Ma, H. (2022). RJX improves wound healing in diabetic rats by modulating systemic inflammation and oxidative stress. *Frontiers in Endocrinology, 13*, 874291. https://doi.org/10.3389/fendo.2022.874291
36. Wang, R., Li, B., Dong, M., Zhu, H., Jin, P., & Zou, Y. (2025). Targeting oxidative damage in diabetic foot ulcers: Integrative strategies involving antioxidant drugs and nanotechnologies. *Burns & Trauma, 13*, tkaf020. https://doi.org/10.1093/burnst/tkaf020 (PubMed)
37. Wang, S., Zhang, Y., Zhong, Y., Chen, L., Li, J., & colleagues. (2024). Reactive oxygen species–scavenging lipid nanoparticle–mRNA formulation promotes diabetic wound healing. *Proceedings of the National Academy of Sciences of the United States of America, 121*(22), e2322935121. https://doi.org/10.1073/pnas.2322935121 (Dove Medical Press)
38. Wu, W., He, Y., Wang, J., Mu, X., Wei, S., Yu, L., & colleagues. (2025). Ligand–metal charge transfer nanozyme with charge–dipole enhancement for diabetic infected wound healing. *Materials Today Bio, 35*, 102516. https://doi.org/10.1016/j.mtbio.2025.102516 (ScienceDirect)
39. Xiao, X., Zhao, F., DuBois, D. B., Liu, Q., Zhang, Y. L., Yao, Q., Zhang, G.-J., & Chen, S. (2024). Nanozymes for the therapeutic treatment of diabetic foot ulcers. *ACS Biomaterials Science & Engineering, 10*(7), 4195–4226. https://doi.org/10.1021/acsbiomaterials.4c00470 (PubMed)
40. Xu, Z., Liu, G., Li, Q., & Wu, J. (2022). A novel hydrogel with glucose-responsive hyperglycemia regulation and antioxidant activity for enhanced diabetic wound repair. *Nano Research, 15*, 5305–5315. https://doi.org/10.1007/s12274-022-4192-y
41. Yadav, P. S., Singh, M., Vinayagam, R., & Shukla, P. (2025). Therapies and delivery systems for diabetic wound care: Current insights and future directions. *Frontiers in Pharmacology, 16*, 1628252. https://doi.org/10.3389/fphar.2025.1628252 (Frontiers)
42. Yi, L. (2024). The regulatory mechanisms of cerium oxide nanoparticles in tissue engineering and regenerative medicine. *Frontiers in Pharmacology, 15*, 1439960. https://doi.org/10.3389/fphar.2024.1439960

43. Zhao, H., Huang, J., Li, Y., Lv, X., Zhou, H., Wang, H., Xu, Y., Wang, C., Wang, J., & Liu, Z. (2020). ROS-scavenging hydrogel to promote healing of bacteria infected diabetic wounds. *Biomaterials*, *258*, 120286. https://doi.org/10.1016/j.biomaterials.2020.120286

44. Zhao, S., Ling, J., Wang, N., & Ouyang, X. (2024). Cerium dioxide nanozyme doped hybrid hydrogel with antioxidant and antibacterial abilities for promoting diabetic wound healing. *Chemical Engineering Journal*, *497*, 154517. https://doi.org/10.1016/j.cej.2024.154517

45. Zhou, B., Duan, Y., Li, W., Chen, T., Wang, J., Cao, M., Lin, G., Yang, K., Lai, Z., & Wu, W. (2025). A tailored hydrogel with local glycemia management, antioxidant activity, and photothermal antibacterial properties for diabetic wound healing. *Advanced Science*, *12*(16), e2414161. https://doi.org/10.1002/advs.202414161